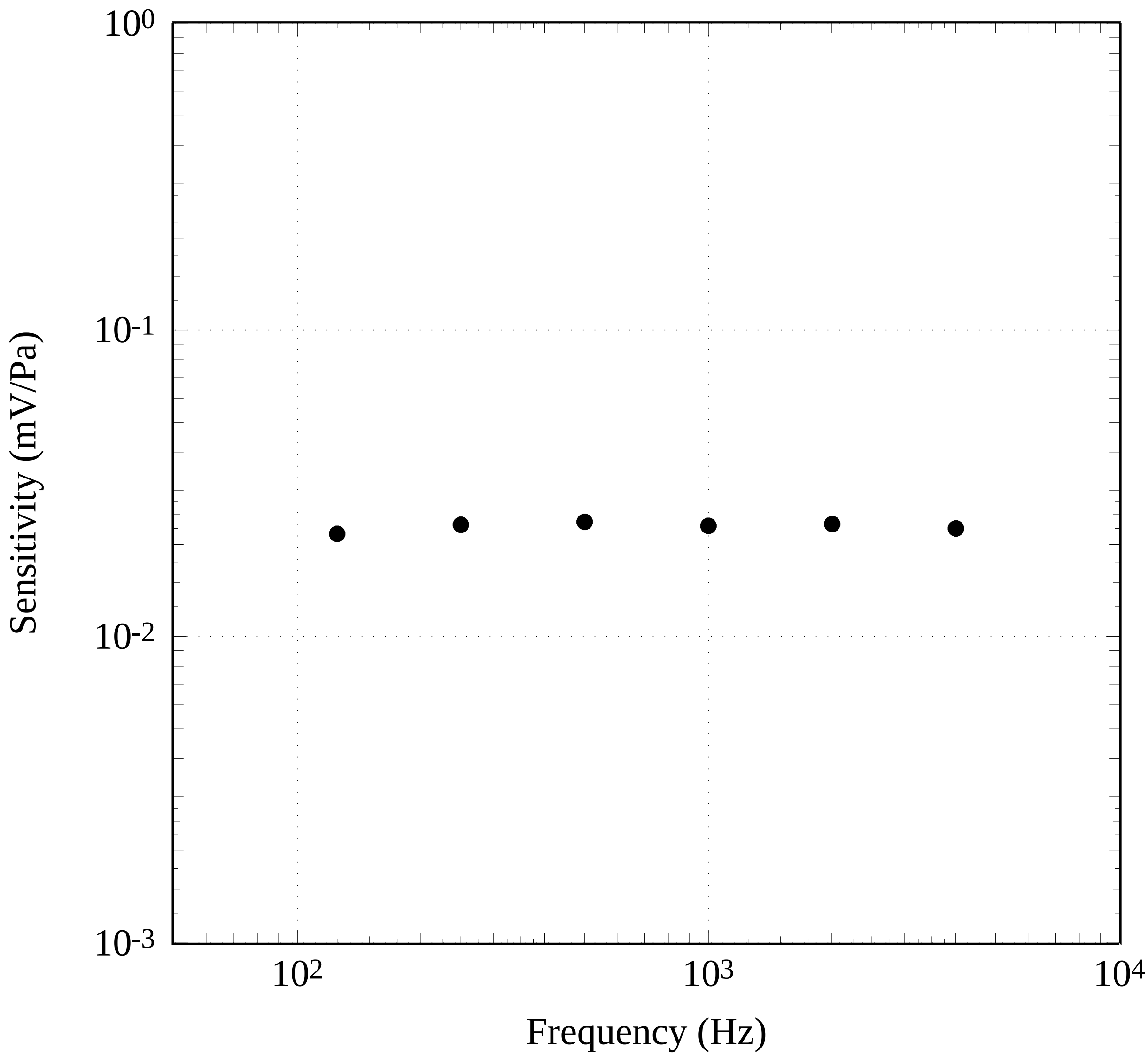

Figure 16. The frequency response of the Endevco 8507-C2 pressure transducer as measured by a GenRad model 1986 Omnical Sound Level Calibrator.

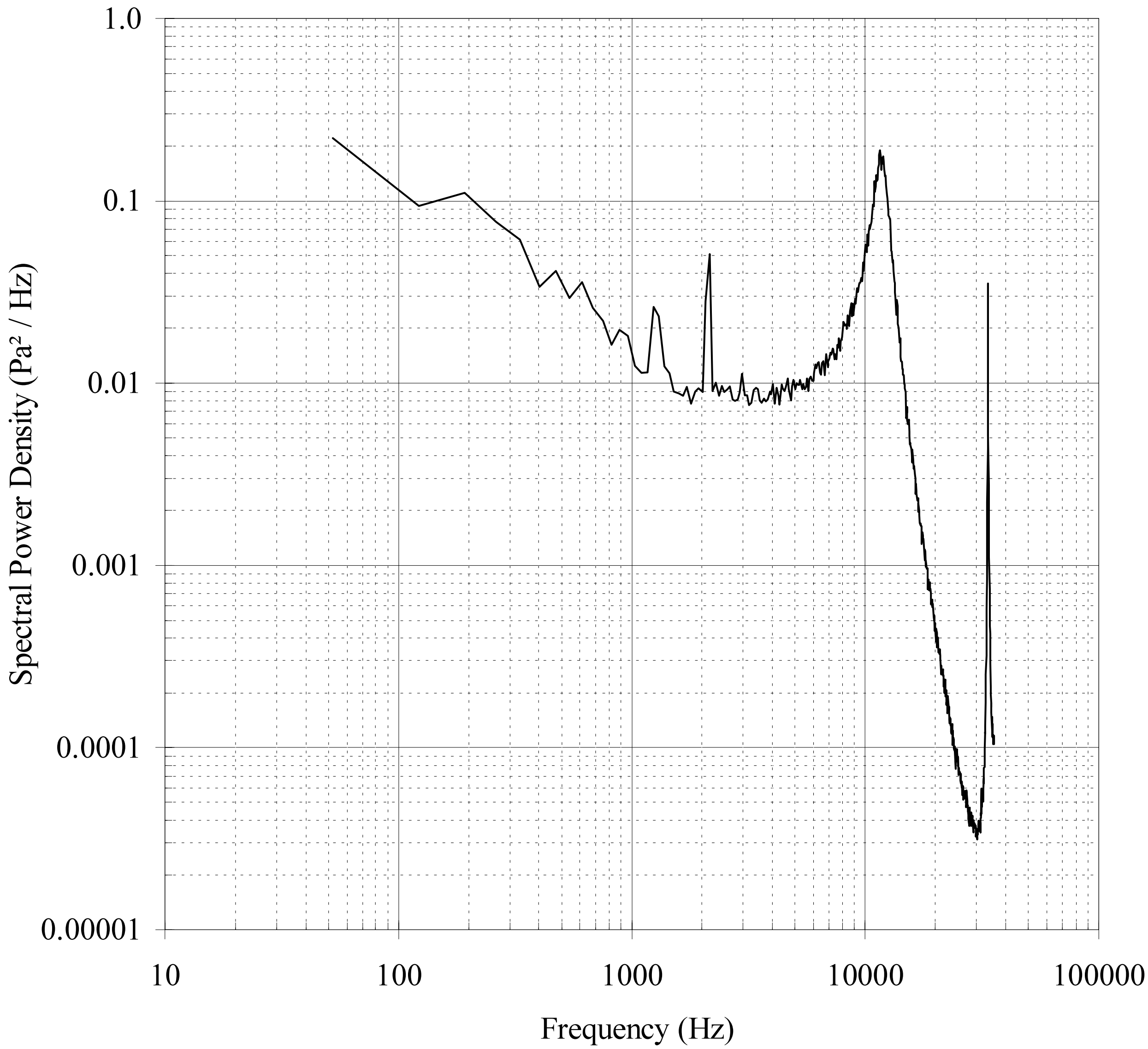

Figure 17. The spectral power density of the pressure transducer signal measured at $x/L = 0.772$, $\phi = 150°$ on a 6:1 prolate spheroid at $\alpha = 10°$ with only the static calibration applied.

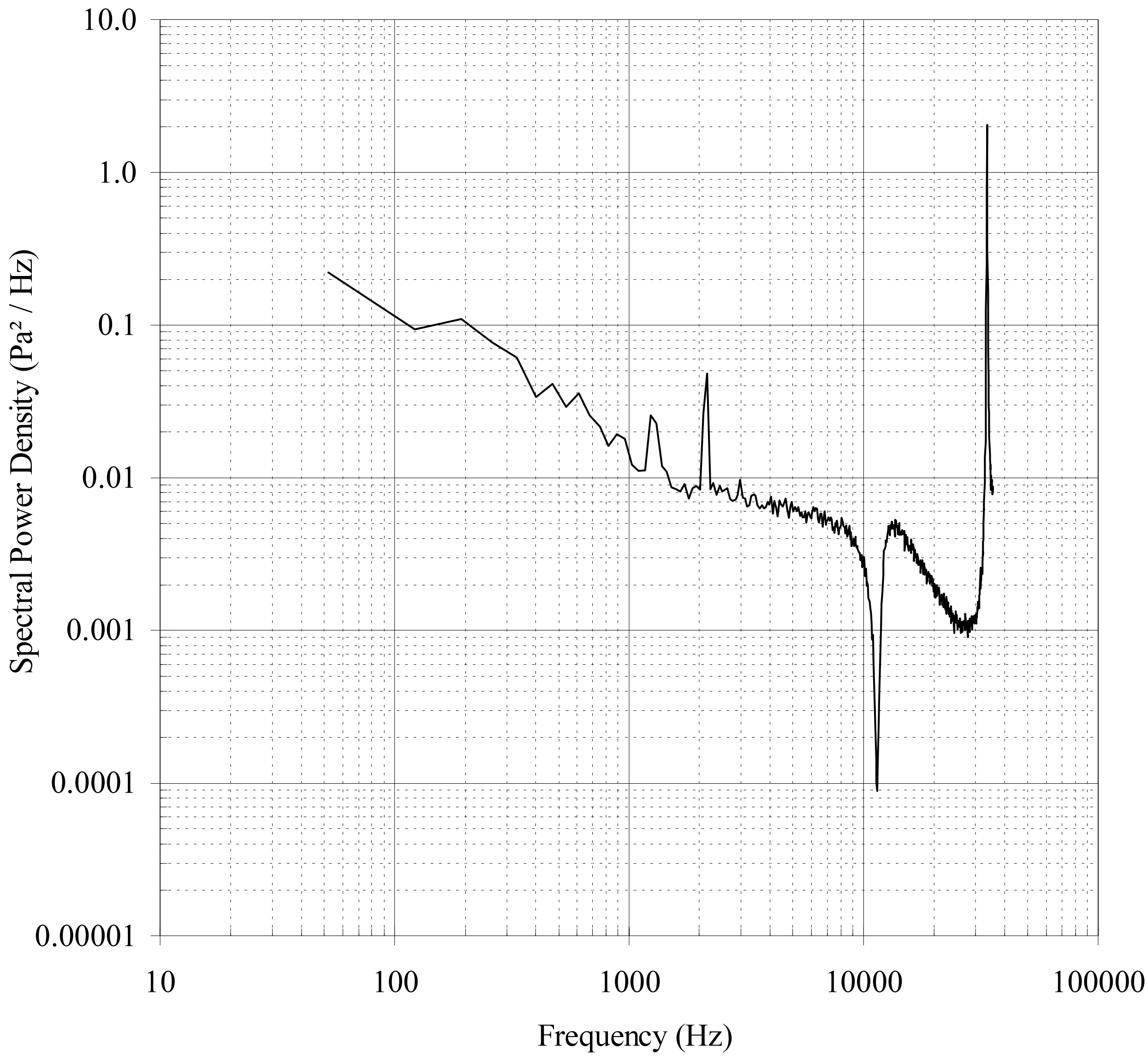

Figure 18. The spectral power density of the pressure transducer signal measured at x/L = 0.772, ϕ = 150° on a 6:1 prolate spheroid at α = 10° with the static calibration and the Helmholtz resonator theoretical correction applied.

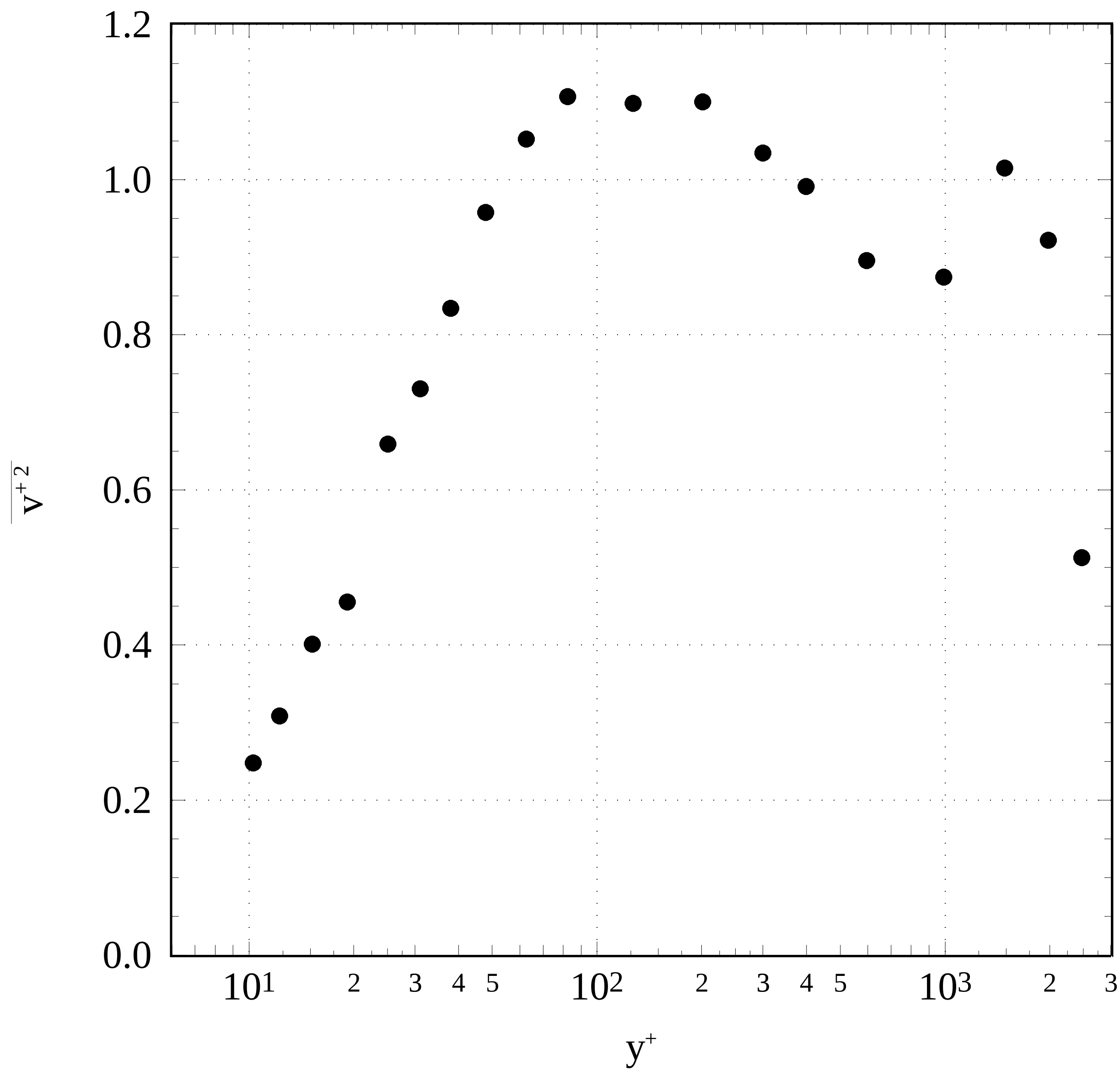

Figure 19. Profile of the $\overline{v^2}/u_\tau^2$ Reynolds normal stress in body-surface coordinates at x/L = 0.772, ϕ = 150° on a 6:1 prolate spheroid at α = 10°. Data of Chesnakas and Simpson (1997).

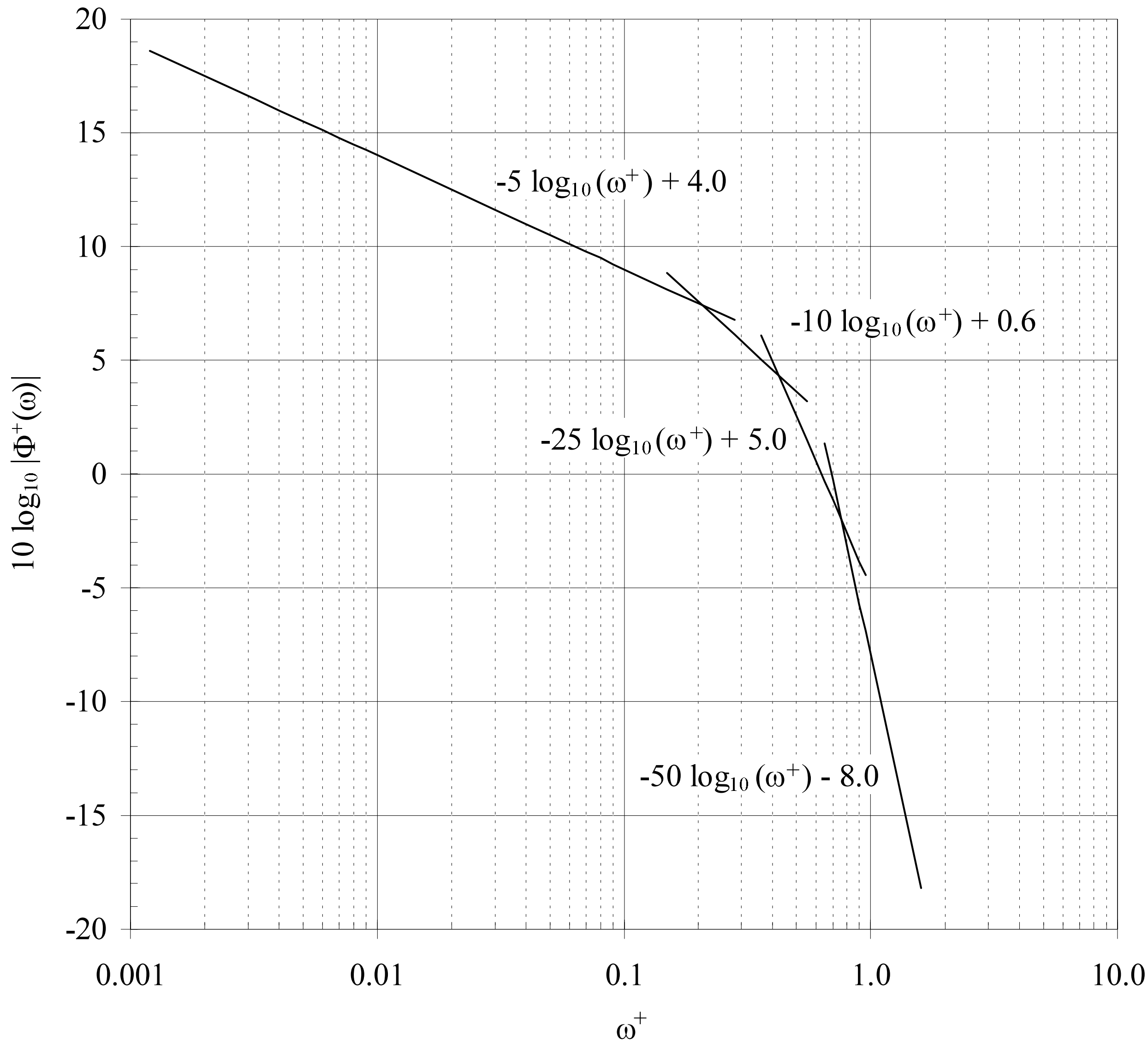

Figure 20. Curves fit to the *p* spectrum beneath a two-dimensional boundary layer with favorable pressure gradient normalized using viscous scales. These curves fit the data of McGrath and Simpson (1987).

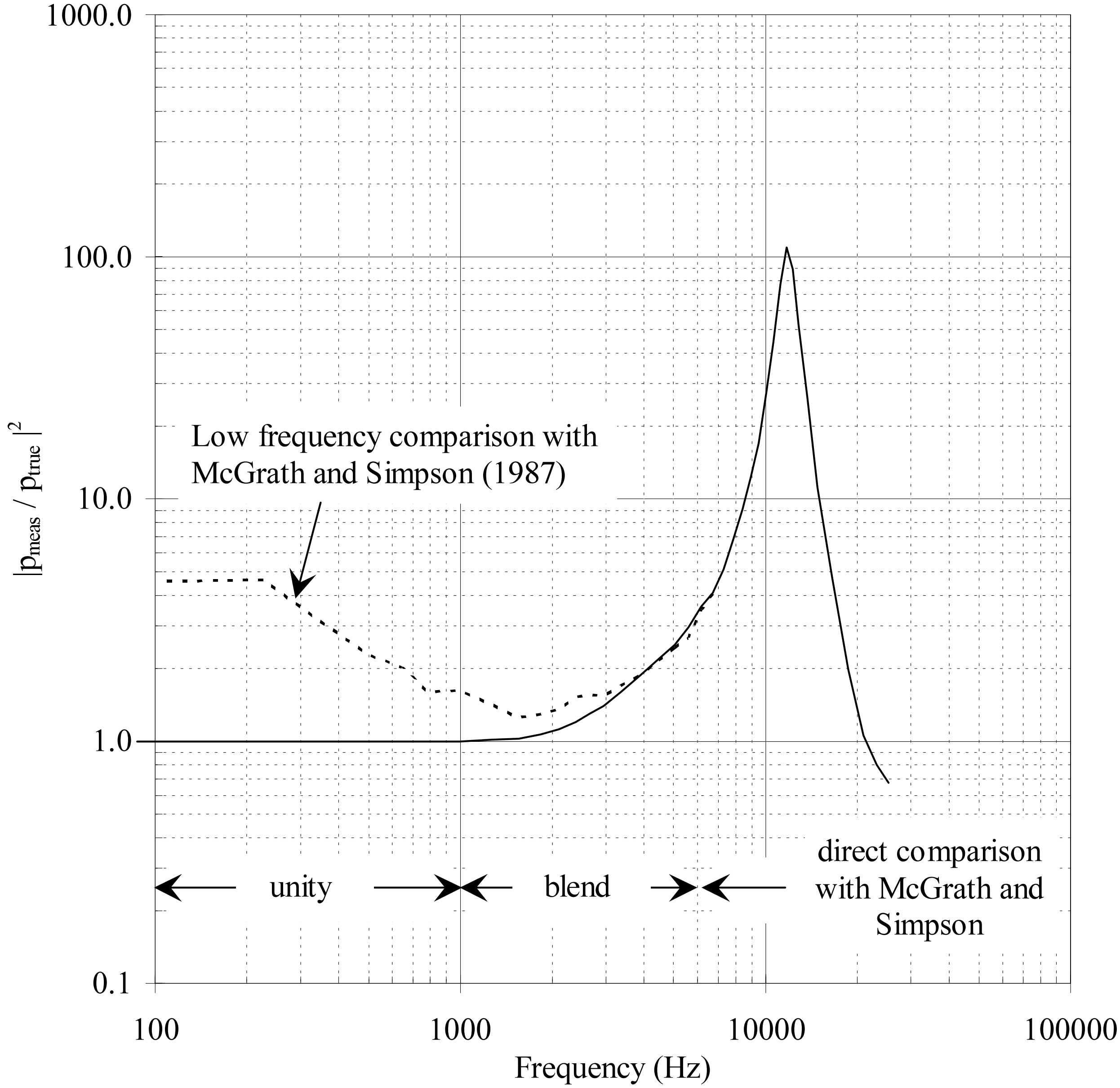

Figure 21. Construction of the approximate transfer function for the Endevco pressure transducer mounted at x/L = 0.772, ϕ = 150° on a 6:1 prolate spheroid at α = 10°.

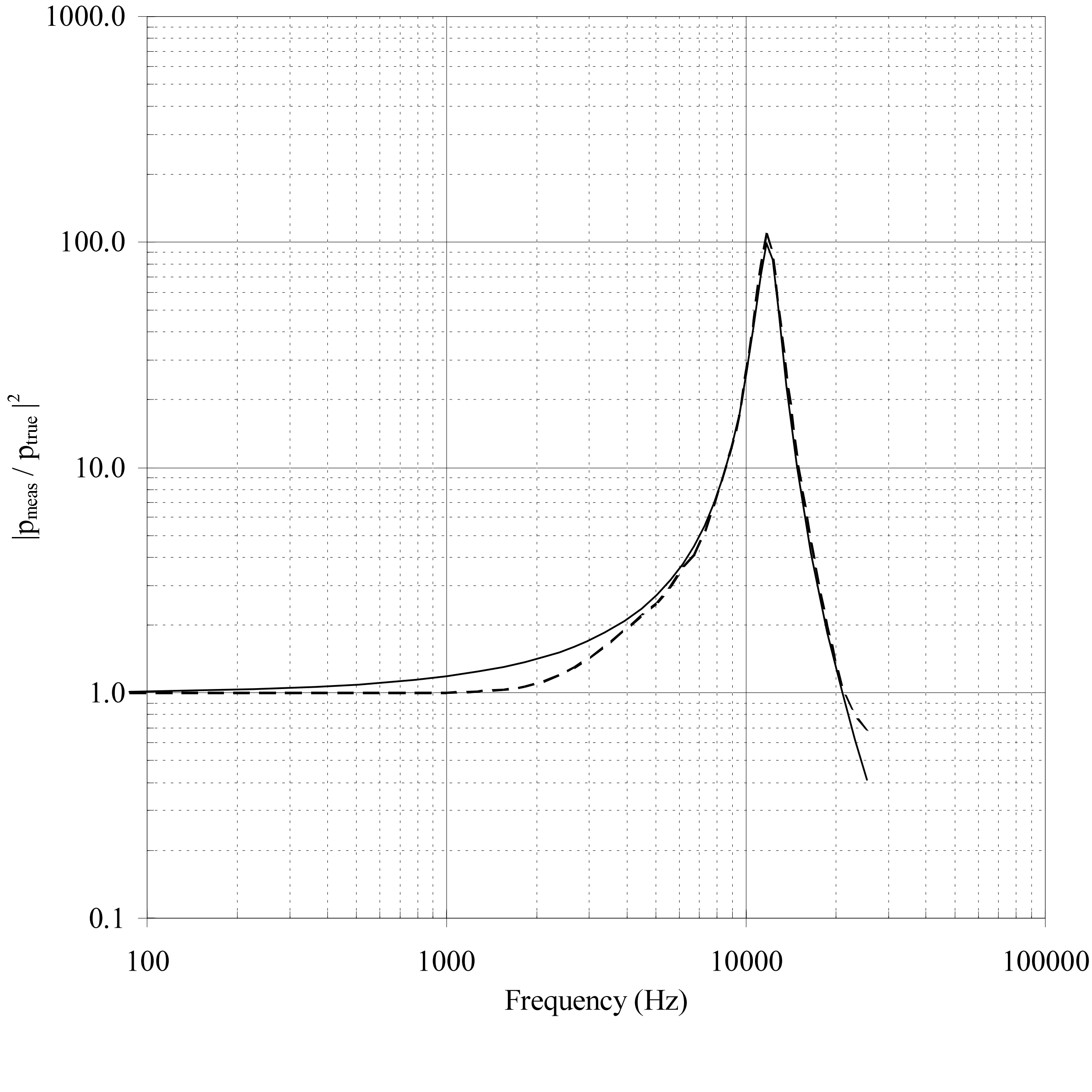

Figure 22. The transfer function used for the *p* spectrum at $\alpha = 10°$, $x/L = 0.772$, $\phi = 150°$ (solid line, equation 43) and the approximate transfer function shown in figure 21 (dashed line).

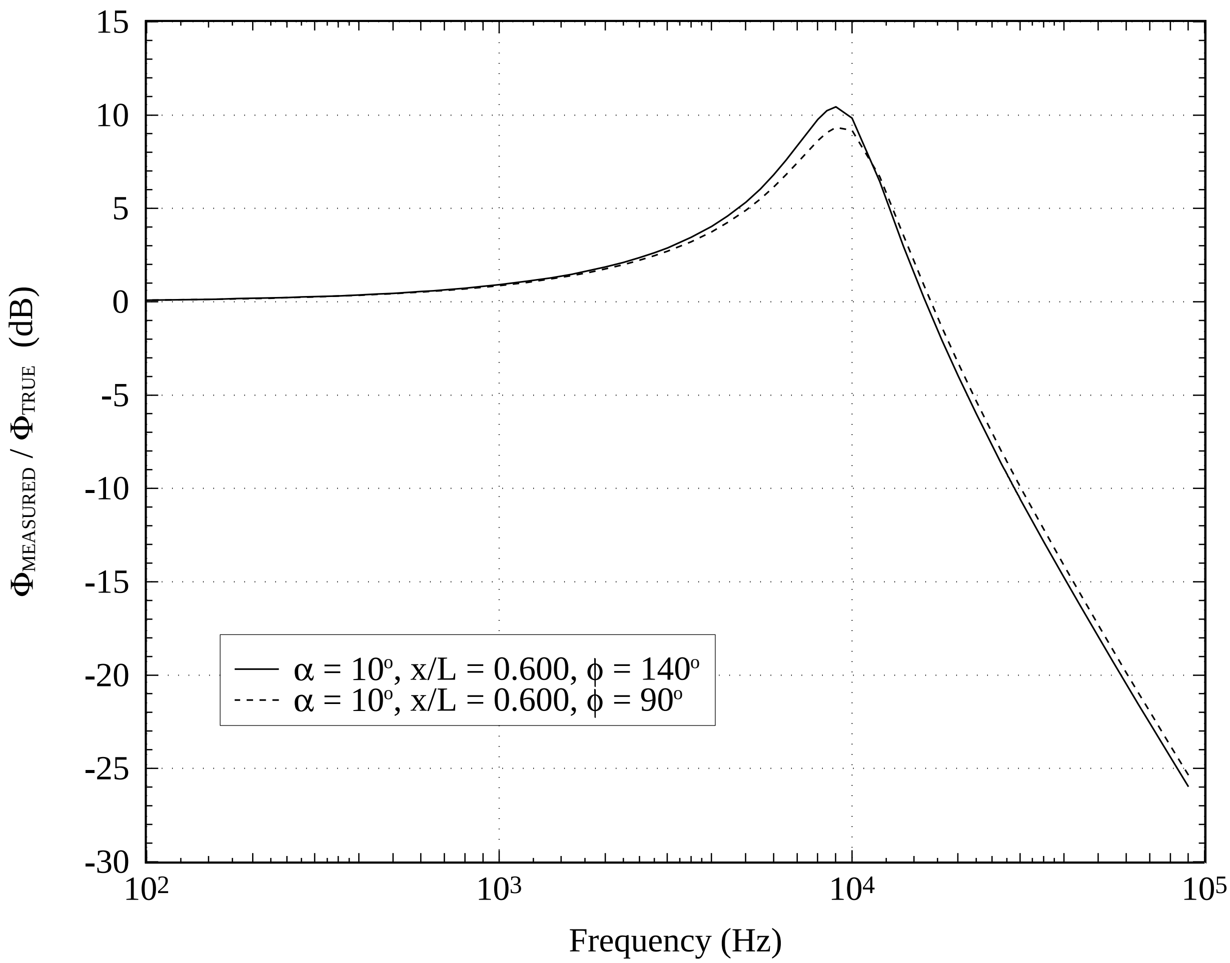

Figure 23. Representative transfer functions that bound the transfer functions that were used for the *p* data at *x/L* = 0.600.

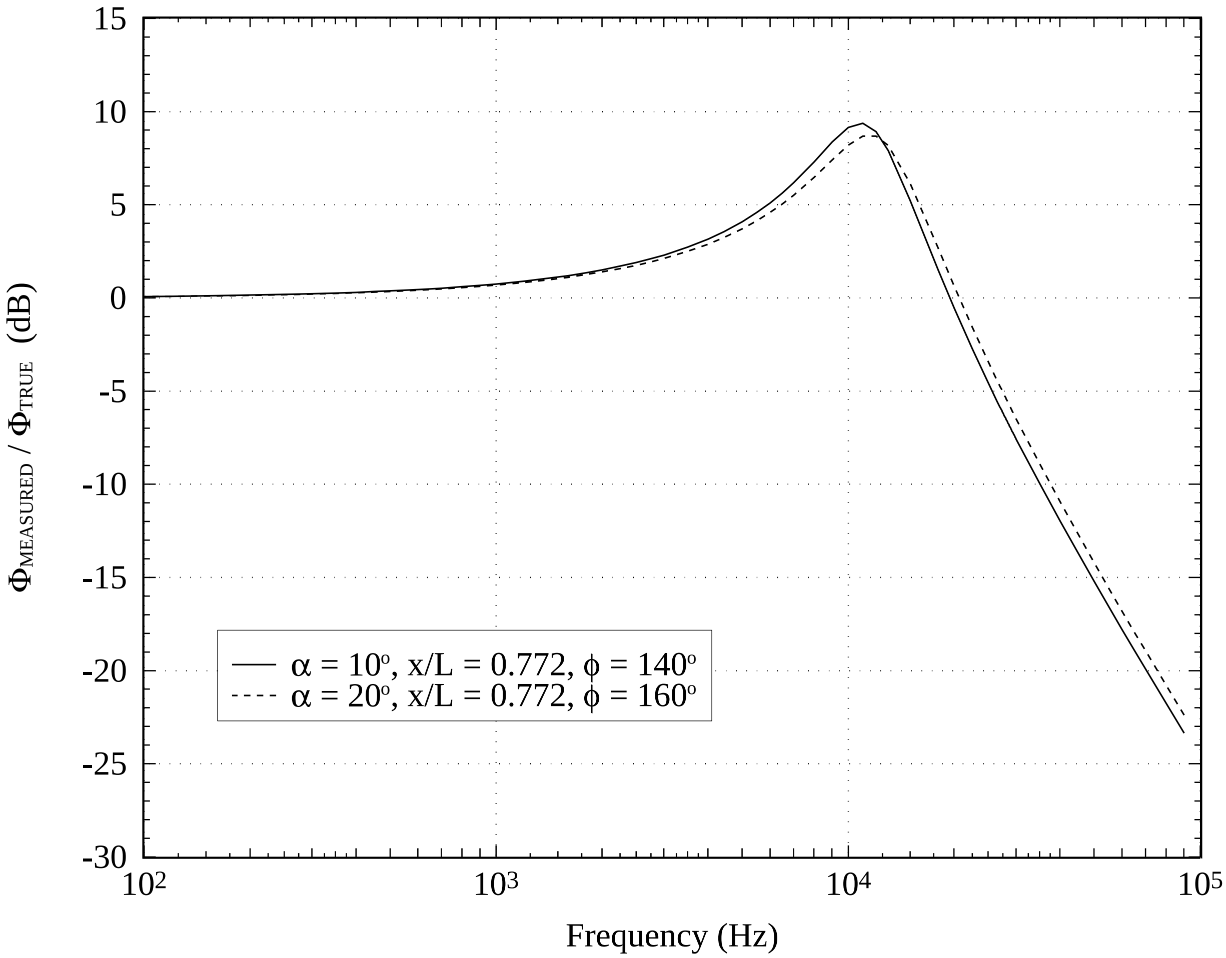

Figure 24. Representative transfer functions that bound the transfer functions that were used for the *p* data at *x/L* = 0.772.